

NEUTRON REFLECTIVITY STUDY OF DIBLOCK FORMATION DURING REACTIVE BLENDING PROCESSES

by

M. Hayashi
Department of Polymer Chemistry
Kyoto University
Kyoto 606-8501, Japan
and
H. Gröll, A. R. Esker,
Li-Piin Sung, Sushil Satija
and **C. C. Han**
National Institute of Standards and Technology
Gaithersburg, MD 20899-8543 USA
and
M. Weber
Polymer Research Laboratory
Engineering Plastics
BASF Aktiengesellschaft,
D-67056 Ludwigshafen, Germany
and
T. Hashimoto
Department of Polymer Chemistry
Kyoto University
Kyoto 606-8501, Japan

Reprinted from *Macromolecules*, Volume 33, No. 17, 6485 -6494, 2001.

NOTE: This paper is a contribution of the National Institute of Standards and Technology and is not subject to copyright.



NIST

National Institute of Standards and Technology
Technology Administration, U.S. Department of Commerce

Neutron Reflectivity Study of Diblock Formation during Reactive Blending Processes

M. Hayashi,[†] H. Grull,^{‡,§} A. R. Esker,^{‡,||} M. Weber,[⊥] L. Sung,[#] S. K. Satija,[#] C. C. Han,[‡] and T. Hashimoto^{*,†}

Department of Polymer Chemistry, Graduate School of Engineering, Kyoto University, Kyoto 606-8501, Japan; Polymers Division and NIST Center for Neutron Research, National Institute of Standards and Technology, Gaithersburg, Maryland 20899; and Polymer Research Laboratory, Engineering Plastics, BASF Aktiengesellschaft, D-67056 Ludwigshafen, Germany

Received January 21, 2000; Revised Manuscript Received June 1, 2000

ABSTRACT: In a series of neutron reflectivity experiments, we studied the fundamental process of diblock formation during reactive blending processes of an immiscible blend comprised of normal polysulfone (hPSU) containing 30% reactive end group-modified deuterated polysulfone (dPSU-R) and polyamide (PA). Diblock formation (dPSU-*b*-PA) and dPSU-R enrichment at the interface between the incompatible polymers were monitored in thin bilayer films using neutron reflectivity. These results are compared to experimental results obtained with bilayer films of pure nonreactive deuterated PSU (dPSU) and PA and pure reactive dPSU-R and PA, respectively. The interfacial width in the pure reactive system is slightly larger than that in the pure nonreactive system, indicating the formation of a diblock copolymer at the interface of the reactive system. The results for the diluted system (30% dPSU-R + 70% hPSU) show an enrichment of the deuterated species at the interface. The amount of dPSU-R at the interface rises from 30 vol % initially, up to an equilibrium value of 47 vol % after annealing at 210 °C within about 30 min. This is interpreted as the formation of diblock copolymer out of the reactive components, dPSU-R and PA, as an interfacial reaction. Annealing at $T = 210$ °C for substantially longer times reveals no further evolution of the interfacial profile, indicating that the diblock, once formed, stays localized at the interface. The formation of a diblock monolayer with complete coverage of the interfacial area is not observed. This is probably due to steric hindrance and strong segregation of the diblock between dPSU-R and PA. The block copolymer layer once formed at the interface suppresses the approach of additional dPSU-R homopolymer toward the interface due to the conformational entropy costs to the homopolymer and block copolymer already at the interface. For these reasons, it is possible to diminish but not eliminate the interfacial tension ($\gamma > 0$) between the PSU and PA, as it is not possible to build up a large enough normalized surface excess, $z^*/R_g < 1$, of dPSU-*b*-PA.

I. Introduction

Polymer blends have been widely used in many industrial applications to design products with specific properties. Blending of different polymers provides a cost-efficient alternative to the synthesis of a new polymer with properties tailored to a specific use. As polymers are usually incompatible, understanding the phase behavior and morphology is of great importance to control phase-separated structures on a mesoscopic scale as well as the mechanical and rheological properties for a desired application. To obtain strong mechanical properties, good adhesion across the interface of the two phases is required. This adhesion in turn is attributed to interpenetration of the component polymer chains across the interface. The degree of interpenetration is controlled by the miscibility of both polymers. Highly miscible polymers will eventually interdiffuse and completely mix, whereas strongly immiscible poly-

mers maintain a sharp interface with a typical observed (or net) interfacial width of $W_{\text{I,obs}} = 2\text{--}5$ nm.^{1–3} The equilibrium intrinsic interfacial width, $W_{\text{I,diffuse}}$, for symmetric polymers with a segmental length l is determined by the miscibility, which can be expressed by the Flory–Huggins interaction parameter χ in the framework of the mean-field theory

$$W_{\text{I,diffuse}} = 2l/(6\chi)^{1/2} \quad (1)$$

for the case of the strong segregation limit ($\chi N \gg 1$).^{4,5} Here, $W_{\text{I,diffuse}}$ is defined as the linearized interfacial thickness given by

$$W_{\text{I,diffuse}} = \frac{\Delta\rho}{|d\rho(z)/dz|_{\text{at } z \text{ satisfying } \rho(z) = \Delta\rho/2}} \quad (2)$$

where $\rho(z)$ is the spatial composition profile of one component along the z -axis normal to the interface and $\Delta\rho$ is the composition difference between the two phases or layers.

Mechanical failures in strongly immiscible binary polymer blends usually occur along the interface between polymer A and polymer B. One way to reinforce resistance against adhesive fracture is to add a diblock polymer consisting of both homopolymers A-*b*-B to the system which will enrich the interfacial region.^{6–11} This block copolymer can either be added as a third component during the blending process^{8,10} or be formed in situ by a chemical reaction during a reactive blending

* To whom correspondence should be addressed.

[†] Kyoto University.

[‡] Polymers Division, National Institute of Standards and Technology.

[§] Present address: Ben-Gurion University of the Negev, Department of Chemical Engineering, PO Box 653, Beer-Sheva 84105, Israel.

^{||} Present address: Virginia Tech, Department of Chemistry, Blacksburg, VA 24061-0212.

[⊥] BASF Aktiengesellschaft.

[#] NIST Center for Neutron Research, National Institute of Standards and Technology.

process.^{12–17} Reactive blending of the usually highly immiscible polymers A and B involves adding a reactive variety of the homopolymers A* and/or B*, which can form in an interfacial reaction either a graft or a block copolymer of A and B. However, an outstanding question is whether a high enough interfacial coverage with diblocks can be achieved during an interfacial reaction to significantly reduce the interfacial tension between the immiscible polymer phases.^{16–21} Understanding the parameters of this reactive blending process, such as the diffusion kinetics of the reactive species within the polymer matrix, as well as the kinetics of the block copolymer formation itself, and of course the diblock localization at the interface with its influence on the interfacial tension of the system, is vital to the subsequent control of product properties.

It is the purpose of this study to explore the interfacial width formed between bilayers of reactive (PSU–R) or nonreactive blends of polysulfone (PSU) and polyamide (PA). Blends of these components might be interesting materials especially for automotive and electrical applications, offering a unique combination of properties such as high heat resistance, good mechanical performance and excellent flow properties. Since polyamides usually offer amino- and carboxylic-end groups, only the polysulfone component has to be modified. From previous investigations it is known that anhydride-terminated polysulfones can react with polyamides in the melt, forming mixtures with finely dispersed small particles.^{22,23} Model experiments using anhydride-terminated polysulfone and amino-terminated polystyrene showed that the conversion of anhydride and amino groups is very fast, even at 60 °C in solution.²⁴ From the size reduction process of mixtures between another polyamide, polyamide 6, and the hydrogenous polysulfone with the same reactive end group used in the present study, PA 6/hPSU–R, one can also conclude that the reaction between PA and dPSU–R should be very fast in the melt.²⁴

This paper reports the results of neutron reflectivity experiments performed on three different thin film bilayer samples. These include Si//dPSU//PA//air, Si//dPSU–R//PA//air and a diluted system of Si//dPSU–R/hPSU//PA//air where “/” is used to indicate a distinct (macroscopic) interface in the sample (i.e.: polymer/substrate interface, polymer/air interface, or polymer/polymer interface) and “/” in dPSU–R/hPSU designates a film composed of a dPSU–R and hPSU mixture. The characters “d” and “h” are used to distinguish between deuterium labeled and regular (“hydrogenous”) polymers; a sketch of the sample geometry is shown in Figure 4a, which will be detailed later in section III.

Generally, three interfaces are present: Si/wafer//polymer A, polymer A//polymer B, and polymer B//air. This study focuses on the polymer//polymer interface. The diluted system offers the possibility to obtain information as to whether the diblock polymer formed during an interfacial reaction stays localized in the interfacial region or diffuses into the PSU- or PA-rich phases.

II. Experimental Methods

II-1. Materials. All polysulfones used for this study were synthesized and characterized by BASF AG, Ludwigshafen, Germany.²⁵ The molecular weights of the samples were determined by light scattering in *N*-methylpyrrolidone (NMP). GPC measurements were performed using THF as the solvent and a polystyrene (PS) calibration curve. The content of end

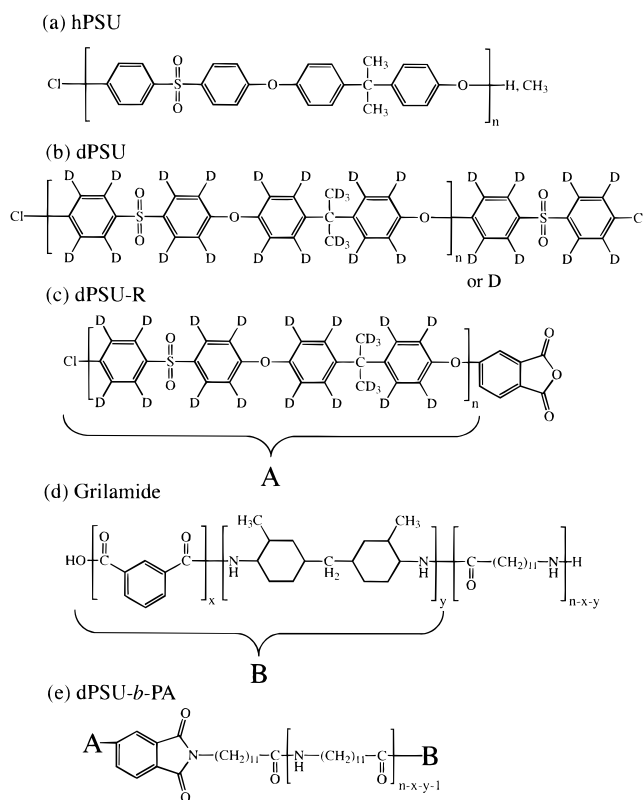


Figure 1. Chemical structures for the polymers studied in this work.

groups was determined by potentiometric titration (OH), elemental analysis (Cl), or IR spectroscopy (anhydride). The glass transition temperatures, T_g 's, of the samples were obtained from DSC-measurements (a DuPont 2000 instrument), which were done in the endotherm mode with a heating rate of 20 K/min. In the obtained DSC traces, T_g was taken as the temperature at which half the increase in heat capacity occurred. The synthetic procedure for the preparation of the polysulfones is given elsewhere.²² For the synthesis of the deuterated samples deuterated monomers were prepared according to the procedures given in the literature.^{26,27} As for polyamide, Grilamide TR 55 LX (EMS Switzerland) was used, which has one amino end group per chain. All data characterizing these samples and the chemical structures are summarized in Table 1 and Figure 1, which also includes dPSU-*b*-PA block copolymer formed by the reaction between dPSU–R and PA.

II-2. Sample Preparation. Uniform polysulfone films (either dPSU, dPSU–R or a mixture of dPSU–R and hPSU) of a thickness d (≈ 600 Å) were prepared by spin-coating on a chlorobenzene solution on silicon wafers (5 mm thick, 75 mm diameter), obtained from Polishing Corporation of America (Santa Clara, CA). Prior to spin-coating, the silicon substrates were cleaned by boiling in a bath of $\text{H}_2\text{O}/30\% \text{NH}_3/30\% \text{H}_2\text{O}_2$ (5:1:1 by volume) and then in a bath of concentrated $\text{H}_2\text{SO}_4/30\% \text{H}_2\text{O}_2$ (70:30, for 1.5 h at $T = 80$ °C). The oxide layer is stripped off using an NH_4F -buffered 3% HF (for 2 min) solution. To obtain a stable hydrophobic surface, the wafer is immersed into a solution of 40% NH_4F . To prepare bilayer samples, a thick film of PA is spin-coated on a second hydrophilic Si wafer out of 1,1,1,3,3,3-hexafluoro-2-propanol (HFIP) solutions (1 wt %). Upon immersing this wafer into water, the PA floats off the wafer onto the water surface and is subsequently picked up with the first wafer. This bilayer specimen is dried at $T = 70$ °C under vacuum for 24 h. In this study, the specimen thus prepared is referred to as the initial state.

The samples were annealed at a temperature $T = 210$ °C which is above the glass transition temperatures of all the component polymers (see Table 1) and subsequently quenched

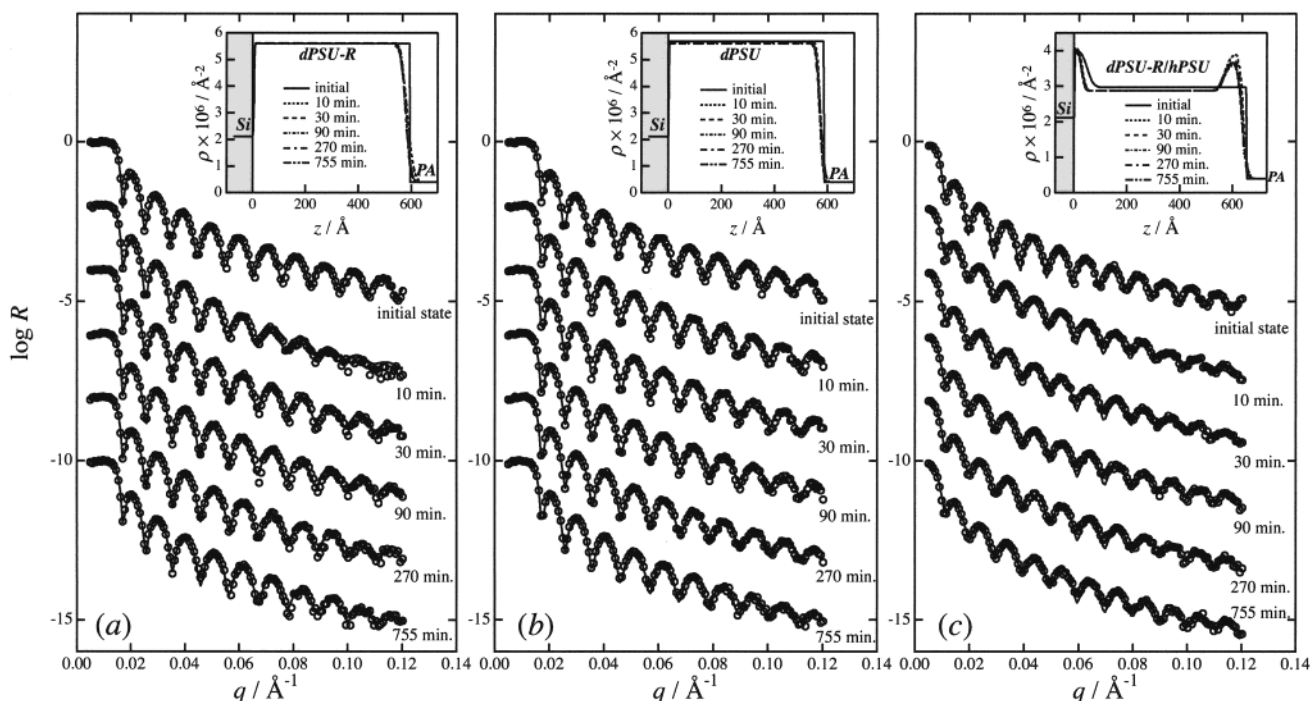


Figure 2. Neutron reflectivity profiles for different annealing times: experimental profiles (○) and the best-fit profiles (—) with the corresponding scattering length density profiles provided as insets. All measurements were performed with the neutron beam entering through the silicon wafer. Key: (a) pure reactive system, Si/dPSU-R/PA/air; (b) pure nonreactive system Si/dPSU/PA/air; (c) diluted reactive system Si/hPSU/dPSU-R/PA/air.

back to room temperature (below T_g for all components) at which the neutron reflectivity measurements were performed.

II-3. Neutron Reflectivity. Neutron reflectivity provides information about the interfacial width with a spatial resolution in the range of 2–8 Å, depending on the experimental conditions, such as q range, film thickness, and neutron scattering length density contrast perpendicular to the film surface.^{11,28} All neutron reflectivity measurements were performed at the horizontal NG7 reflectometer at the National Institute of Standards and Technology (NIST), Gaithersburg, MD. A well collimated neutron beam of a fixed wavelength ($\lambda = 4.76$ Å) is reflected on the sample surface. The neutron momentum (e.g., magnitude of the scattering wave vector q , $q = (4\pi/\lambda) \sin \theta$; θ , incident and reflection angle) is varied by changing the angle of incidence typically over a range from 0 to 3° with an incoming beam through the silicon substrate. The reflected beam intensity is measured using a pencil neutron detector. Here, only the specular reflection is considered, where the incident beam, reflected beam, and the film normal are in one plane and the reflection angle is the same as the angle of incidence. The specular reflected beam intensity was corrected for the background intensity for further analysis.²⁹

The neutron reflectivity data were fitted using a standard multilayer fitting routine for scattering length densities (SLD).²⁹ Fit parameters were the SLD of silicon, the silicon/polysulfone (PSU: either dPSU-R, dPSU, or dPSU-R/hPSU) roughness, the thickness and SLD of the PSU layer, the interfacial width between the PSU layer and the PA layer, and the thickness and SLD of the PA layer. For the SLD of silicon a well-established standard value was used (2.11×10^{-6} Å⁻²), the silicon/PSU layer roughness was determined for the corresponding single layer film using X-ray and/or neutron reflectivity. The SLD of the PSU layer was calculated to be 5.61×10^{-6} Å⁻² for dPSU or dPSU-R (defined hereafter as ρ_{dPSU}) and 2.98×10^{-6} Å⁻² for dPSU-R/hPSU (defined hereafter as $\rho_{\text{dPSU-R/hPSU}}$), and the SLD of the PA layer was calculated to be 3.98×10^{-7} Å⁻² (defined hereafter as ρ_{PA}). The thickness of the PA layer was set at 5000 Å, the value of which hardly affects the calculated reflectivity curve for the fitting. Thus, the remaining important parameters to be determined

from the fitting procedure are the thickness of the PSU layer and the interfacial width between the PSU layer and the PA layer. Fortunately they are determined more or less independently from each other in the fitting procedure of the reflectivity curve, because the former primarily affects the width of the interference fringes and the latter affects the decay of the maximum intensity of each fringe with q .

The SLD profiles across the interface between the PSU and PA layers for the undiluted reactive system and the nonreactive system were assumed to be given by a convolution product of a function $\rho_f(z)$ and a Gaussian function with a standard deviation σ

$$h(z) = (2\pi\sigma^2)^{-1/2} \exp(-z^2/2\sigma^2) \quad (3a)$$

$\rho_f(z)$ in this case is given by a step function

$$\rho_f(z) = \begin{cases} \rho_{\text{dPSU}} (\text{const.}) & \text{for } z \leq T_{\text{PSU}} \\ \rho_{\text{PA}} (\text{const.}) & \text{for } z > T_{\text{PSU}} \end{cases} \quad (3b)$$

where T_{PSU} is the thickness of the PSU layer.

The SLD profiles across the interface between the PSU and PA layers for the diluted reactive system were to be given again by a convolution product of $\rho_f(z)$ in eq 3b and $h(z)$ but $\rho_f(z)$ in this case should take into account the occurrence of interfacial enrichment by dPSU-R or dPSU-R/hPSU. In this work $\rho_f(z)$ was assumed to be given by the following function derived for polymer brushes grafted on a planar wall under Θ conditions³⁰

$$\rho_f(z) = \begin{cases} \rho_{\text{dPSU-R/hPSU}} (\text{const.}) & \text{for } z \leq T_{\text{PSU}} - H_{10} \\ \rho_{\text{dPSU-R/hPSU}} + \varphi_{10}^{(m)} \left[1 - \frac{(z - T_{\text{PSU}})^2}{H_{10}^2} \right]^{1/2} & \text{for } T_{\text{PSU}} - H_{10} \leq z \leq T_{\text{PSU}} \\ \rho_{\text{PA}} (\text{const.}) & \text{for } z > T_{\text{PSU}} \end{cases} \quad (3c)$$

where $\rho_{\text{dPSU-R/hPSU}}$, $\varphi_{10}^{(m)}$, and H_{10} were treated as adjustable parameters and the latter two quantities describe the amount and the length scale for the enrichment, respectively.

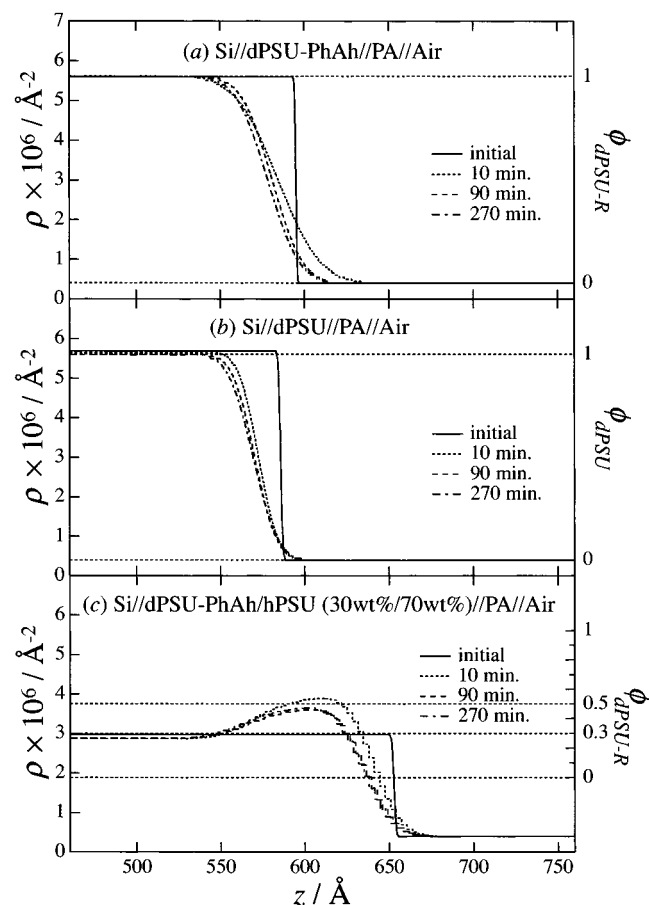


Figure 3. Interfacial profiles for (a) the pure reactive, (b) the pure nonreactive, and (c) the diluted reactive systems. The left axes correspond to the scattering length density, while the right axes indicate the volume fraction of deuterated species ϕ_{dPSU} or $\phi_{\text{dPSU-R}}$. dPSU-PhAh in (a) and (c) denotes dPSU-R. When the profiles in (c) refer to $\phi_{\text{dPSU-R}}$ (the right ordinate axis), the profiles have a physical meaning only z -range satisfying $\phi_{\text{PA}}(z)$ (volume fraction of PA at $z \approx 0$ (i.e., $z \leq 650$ Å for the initial state, 610 Å for the 10 min after the annealing and 604 Å for the 90 and 270 min after the annealing).

Then the linearized interfacial thickness $W_{\text{I,obs}}$ obtained from the SLD profile is given by eq 4, for both the undiluted and diluted systems as well as for the diluted reactive system

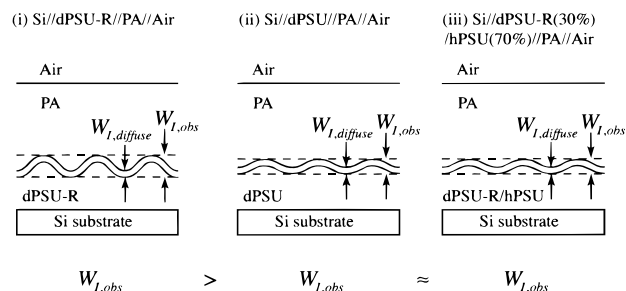
$$W_{\text{I,obs}} = \sqrt{2\pi}\sigma \quad (4)$$

where σ_1 is the corresponding standard deviation σ from eq 3a.^{31–33}

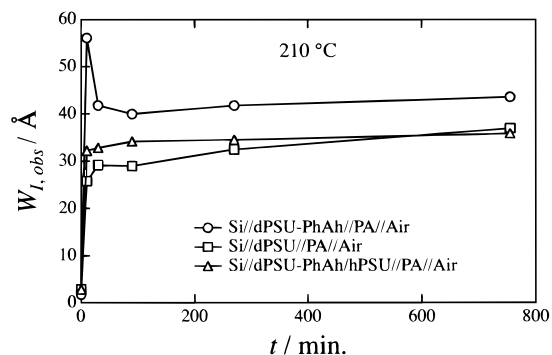
Generally, standard NR measurements do not provide unique information about SLD profiles because there is no simple relationship between the real space profile and the reflection intensity.³⁴ Nevertheless, all fits are very sensitive to the interfacial width at the polymer/polymer interface although, out of principle, it can never be ruled out that other SLD profiles can fit the NR data equally well especially for the more complicated profiles.^{34–36}

III. Experimental Results

Figure 2 shows typical NR data for several different annealing times and systems at $T = 210$ °C. The experimental data and their corresponding SLD profiles provided in the insets represent the pure reactive end-group-labeled polysulfone Si//dPSU-R//PA//air (part a), the pure nonreactive Si//dPSU//PA//air (part b), and the diluted reactive system Si//hPSU/dPSU-R//PA//air (part c). The sample geometries are shown schematically in



(a) Schematic illustrations for sample geometries



(b) Time dependence of the interfacial widths at 210 °C

Figure 4. (a) Schematic representation of the sample geometries and the results for the equilibrium interfacial widths. (b) Interfacial widths as a function of annealing time at $T = 210$ °C for the three systems: Si//dPSU-R//PA//air, Si//dPSU//PA//air, and Si//dPSU-R/hPSU//PA//air. dPSU-PhAh denotes dPSU-R.

Table 1. Characteristics of Polymers Used in This Study

polymer	N_w	N_w/N_n	endgroup (%)				T_g (°C)
			PhAh	OH	Cl	OCH ₃	
hPSU ^a	86	2.52			50	50	188
dPSU ^b	58	3.51		3	97	50	176
dPSU-R ^c	80	6.27	50	35	15		174
PA ^d	3.3×10^4 ^e	3.90					113

^a Protonated polysulfone. ^b Deuterated polysulfone. ^c Deuterated polysulfone with phthalic anhydride group. ^d Polyamide, Grilamide, EMS, Switzerland. ^e Since an average degree of polymerization is not well defined, we indicated the weight-average molecular weight obtained from GPC (using HFIP as solvent) instead.

Figure 4a and will be described in detail later in this section. At early annealing times for all experiments, a shrinking of the bottom polysulfone (PSU) (either dPSU-R, dPSU, or dPSU-R/hPSU) layer by 15 Å (corresponding to ≈ 2.5 vol %) occurs, which can be related to fast diffusion by a certain amount of a low molecular weight fraction present in all the PSU samples into the PA layer. It should be noted that the thinning of the total PSU thickness does not complicate the NR analysis stated earlier in section II-3. In an additional NR experiment (results not presented here) with a bilayer of oligomeric dPSU//PA at $T = 160$ °C, it was determined that low molecular weight dPSU shows a considerably higher miscibility with PA than the strongly incompatible high molecular weight dPSU. The estimated amount of low molecular weight impurity (≈ 2.5 vol %) described above is consistent with the fraction of low molecular weight dPSU determined by GPC analysis. It is assumed that the interdiffusion of this small amount of low molecular weight PSU impu-

Table 2. Time-Dependent Changes of the Parameters:
 $\varphi_{10}^{(m)}$, H_{10} , $\rho_{\text{dPSU/hPSU}}$, T_{PSU} , $W_{\text{I,obs}}$, and z^*

time (min)	$\varphi_{10}^{(m)}$ $\times 10^5 (\text{\AA}^{-2})$	H_{10} (\AA)	$\rho_{\text{dPSU-R/hPSU}}$ $\times 10^4 (\text{\AA}^{-2})$	T_{PSU} (\AA)	$W_{\text{I,obs}}$ (\AA)	z^* (\AA ⁻¹)
0			1.50	650	2.86	
10	5.76	80.8	1.44	635	32.3	15.1
30	4.73	79.8	1.45	633	32.8	11.5
90	4.19	79.6	1.45	631	34.2	9.48
270	4.43	80.1	1.45	629	34.5	10.3
755	4.68	74.2	1.45	629	35.9	9.75

rity does not affect the results at long annealing times but may well influence the interfacial width at early annealing times.

This analysis focuses on the comparison of the interfacial profiles and widths in all three systems between the PSU and PA layers. Compared to the initial state, the interfacial width $W_{\text{I,obs}}$ between the PSU and PA layer increases at early annealing times and eventually reaches an equilibrium value. The width $W_{\text{I,obs}}$ was determined by fitting the first derivative of the ρ profile with respect to z with a Gaussian function $h(z)$ given by eq 3a, with $W_{\text{I,obs}}$ then given by eq 4.

Figure 3 shows the SLD profiles (left ordinate axes) for the undiluted reactive system (a) and undiluted nonreactive system (b) as well as the reactive system diluted with hPSU (c) as a function of time. The characteristic parameters evaluated for the diluted system were summarized in Table 2. The SLD profiles for the undiluted systems (Figures 3a and 3b) were converted to their corresponding volume fraction profiles for (a) dPSU-R ($\phi_{\text{dPSU-R}}$), or (b) dPSU (ϕ_{dPSU}), using the relation $\rho = \rho_{\text{dPSU-R}}\phi_{\text{dPSU-R}} + \rho_{\text{PA}}\phi_{\text{PA}}$ with $\rho_{\text{dPSU-R}} = 5.61 \times 10^{-6} \text{ \AA}^{-2}$ for both dPSU-R and dPSU and $\rho_{\text{PA}} = 0.398 \times 10^{-6} \text{ \AA}^{-2}$, as shown on the right ordinate axes in Figure 3, parts a and b. For the diluted system Si//dPSU-R/hPSU//PA//air (Figure 3c) this conversion is only valid under the assumption that no PA is present in the hPSU/dPSU-R layer: $\rho = \rho_{\text{dPSU-R}}\phi_{\text{dPSU-R}} + \rho_{\text{hPSU}}\phi_{\text{hPSU}}$ with $\rho_{\text{dPSU-R}} = 5.61 \times 10^{-6} \text{ \AA}^{-2}$ and $\rho_{\text{hPSU}} = 1.89 \times 10^{-6} \text{ \AA}^{-2}$. When the profiles in Figure 3c refer to $\phi_{\text{dPSU-R}}$ (the right ordinate axis), the profiles have a physical meaning only in z -range satisfying $\phi_{\text{PA}}(z)$ (volume fraction of PA at $Z \approx 0$ (i.e., $z \lesssim 650 \text{ \AA}$ for the film in the initial state, 610 \AA for that at 10 min, and 604 \AA for that at 90 and 270 min after the annealing). A comparison of the profiles for different annealing times shows that the equilibrium interfacial width is reached within ≈ 10 min of annealing and does not evolve further even for very long annealing times. The undiluted reactive system Si//dPSU-R//PA//air shows the largest equilibrium interfacial width $W_{\text{I,obs}}$ compared to the undiluted nonreactive and the diluted reactive systems. The latter two systems have almost identical $W_{\text{I,obs}}$. These findings are schematically shown in Figure 4a. Figure 4b shows the time dependence of the interfacial width for all three experiments.

To obtain information about the diffusion time of the reactive species dPSU-R in the matrix of PSU, an interdiffusion experiment with a bilayer of dPSU-R//hPSU was performed. For this purpose, a dPSU-R film with a thickness of about 500 \AA is spin-coated on a silicon wafer (same cleaning procedure as above) and a 700 \AA thick film of hPSU is floated on top to prepare a bilayer film of air//hPSU//dPSU-R//Si. The interdiffusion is studied in a series of annealing ($T = 210^\circ\text{C}$)/quench experiments using NR as well. Figure 5 shows the reflectivity and the SLD profiles used to fit the data.

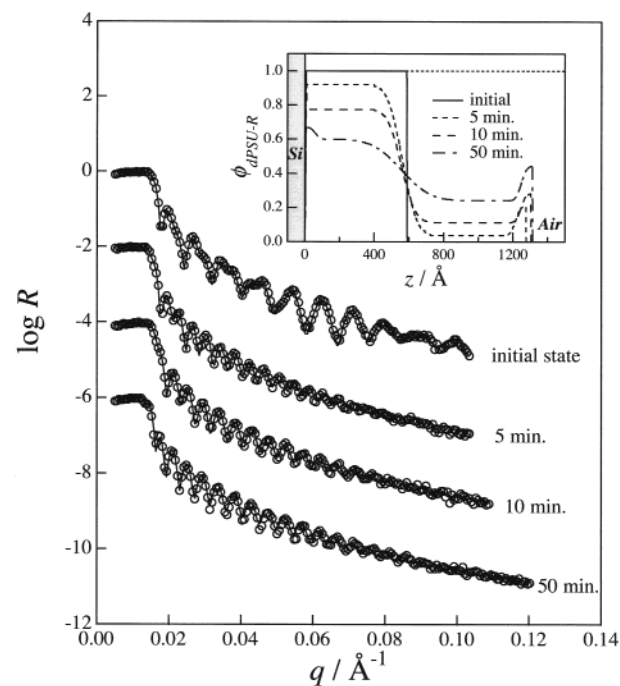


Figure 5. Bilayer interdiffusion experiment using hPSU and dPSU-R at $T = 210^\circ\text{C}$. The SLD profiles used to model the data are shown in the inset. The beam for the neutron reflectivity experiments was incident from air. Key: (○) experimental profiles; (—) the best-fit profiles with the SLD profiles shown in the inset.

During early annealing times a rapid interdiffusion is observed, leading to a broadening of the initial interface with time, which can be modeled using ordinary error-functions. Furthermore, a drop of the SLD plateau in the dPSU-R layer and an increase of the SLD plateau in the hPSU layer is observed even at the early stages (5 min annealing). It is also possible to explain this observation by considering the rapid interdiffusion of low molecular weight components included in the hPSU and the dPSU-R. The deuterated component adsorbs at the air interface forming a layer of deuterated polymer. The interfacial width, which is extracted in the same way as described above, can be used to determine the mutual diffusion coefficient of the system hPSU//dPSU-R by plotting the squared interfacial width vs annealing time.³⁷

$$W_{\text{I,obs}}^2 = 2\pi(\sigma_0^2 + 2Dt) \quad (5)$$

The mutual interdiffusion coefficient D is determined from the slope of a linear fit of eq 5 to the data with $D = (3.42 \pm 0.27) \times 10^{-16} \text{ cm}^2/\text{s}$. $W_{\text{I,0}} \equiv \sqrt{2\pi}\sigma_0$ is the initial interfacial width of the bilayer before the onset of interdiffusion, and σ_0 is the initial value of σ in eq 3a. More rigorously, D seems to depend on composition and time as well, which may be analyzed based on the Boltzmann–Matano analysis³⁸ and an analysis shown by Schewmon,³⁹ respectively. However these analyses are beyond the scope of the present paper.

IV. Discussion

IV-1. Time Dependent Changes in the Interfacial Profile. Figure 3 shows in detail the time dependent change of the interfacial profile for the systems with the pure reactive system (a), the pure nonreactive system (b), and the diluted reactive system which contained

30% reactive end group-labeled deuterated dPSU-R (c), respectively. As mentioned previously, the shrinking of the total PSU layer thickness can be related to the presence of a low molecular weight PSU fraction which is considerably more miscible with PA than high molecular weight PSU. The large temporary increase in the interfacial width observed at the first annealing time (10 min) in the pure reactive system might be due to the interdiffusion of low molecular weight impurities at early annealing times which just happened to be captured in the initial quench step. Another possible explanation is a temporary long wavelength undulation of the interface triggered by the fast interdiffusion of the low molecular weight species. The latter possibility is currently being investigated by performing similar experiments using low molecular weight hPSU designated low-hPSU.⁴⁰ Unfortunately, specular neutron reflectivity on the present system does not offer any possibility to distinguish between these two scenarios.⁴¹

Large-scale undulations of the interfacial plane as mentioned above are also possible when the amount of diblock present in the system is in excess of what is required to saturate the interface driving the interfacial tension γ between the two polymer phases to zero. For $\gamma \approx 0$ the increase in interfacial area, dA , due to an undulating interfacial plane is not penalized by an increase in free energy ($dG = \gamma dA$). The required normalized surface excess of diblock polymer, z^*/R_g , to substantially diminish γ , where R_g is the radius of gyration for the principal block, is assumed to be larger than a critical threshold, which is on the order of $z^*/R_g = 1.0$ – 2.5 .⁴² Systems forming microemulsions with no interfacial tension ($\gamma = 0$) between the phases in the presence of added diblock serve as examples where this is possible.⁴³ As we will discuss shortly, in the context of existing theories,^{16–21} it is believed that a reactive blending system leading to diblock formation at the interface between two immiscible polymers will not exceed the critical threshold. Under these conditions, $z^*/R_g < 1$, a sharp interface should be maintained. In contrast, recent experimental work with a graft system shows that it is possible to exceed this threshold and induce extensive broadening at the interface.^{16,17}

IV-2. Analysis of the Interfacial Width and Localization of Block Copolymers Formed at the Interface. Before extending the discussion to a detailed analysis of the interfacial width for the PSU//PA system, it should be emphasized that the experimental value $W_{I,obs}$ obtained by neutron reflectivity is the apparent interfacial width consisting of two different components: the intrinsic interfacial width due to interpenetration of polymer chains (or chain ends) across the interface $W_{I,diffuse}$ and a contribution of thermally excited capillary waves $W_{I,capillary}$ leading to a long-ranged waviness of the planar interface.

$$W_{I,obs}^2 = W_{I,capillary}^2 + W_{I,diffuse}^2 \quad (6)$$

The experimentally observed interfacial width is the average over the neutron beam footprint area (ca. 4 cm \times 3 cm). The contribution of capillary waves was neglected in the initial mean-field treatment by Helfand^{4,5} leading to theoretical $W_{I,diffuse}$ values that are smaller than the observed value for the polymer/polymer interfacial width. Shull et al. and Semenov extended earlier work done on capillary waves⁴⁴ to polymer blends to account for the contribution of capillary waves at the interface.^{45,46}

All three experiments show that the equilibrium interfacial width $W_{I,obs}$ is obtained after very short annealing times (on the order of 10–30 min) as seen in Figure 4b. The observed trend in $W_{I,obs}$ hardly changing with time after 30 min for the diluted system is not due to diffusion-limited behavior of dPSU-R in the polysulfone layer. This is clearly shown by bilayer interdiffusion experiments of dPSU-R/hPSU at 210 °C with neutron reflectivity as presented in Figure 5. As seen in the time dependent change of the SLD profile, the interdiffusion is almost complete within 50 min. Hence any changes in the interfacial profiles or interfacial widths in the experiments shown in Figures 3 and 4, if they occurred, should happen within 50 min for our experimental conditions. Thus, the observed values of $W_{I,obs}$ after 50 min should essentially reflect the equilibrium values (Figure 4).

The initial interfacial width of all samples was of comparable magnitude ($W_{I,obs} = 5$ Å).⁴⁷ In all the systems studied in this work, we did not subtract the initial roughness measured after annealing at temperatures above T_g 's for various time periods. This is simply because the initial interface would have no effect on the observed interface once the bilayer film is annealed to reach a thermodynamically stable interfacial width.

The pure reactive system shows the biggest equilibrium interfacial width of $W_I \approx 40$ Å, which can be related to the formation of dPSU-*b*-PA diblock copolymer chains at the interface. As only reactive end-group-labeled polymers, dPSU-R, are present, it is reasonable to assume that the interface is essentially fully covered with dPSU-*b*-PA diblock copolymer chains with an equilibrium number of the block copolymer chains per unit of interfacial area. An excess number of block chains will cost stretching free energy of the block chains and hence be unlikely to form.

In this system, diffusion of the diblock from the interface toward the interior of the dPSU-R layer can be excluded, as this diffusion should cause a decrease of the SLD of the dPSU-R layer, which is not observed in Figure 3a. Note that the dPSU-*b*-PA has a lower SLD than pure dPSU-R. A significant diffusion of dPSU-R into the PA layer can also be excluded, as this would cause steady shrinking of the dPSU-R layer. Instead, the shrinking of the dPSU-R layer ceases after about 90 min of annealing, as seen in Figure 3a. Only a small amount (2.5 vol %) of the very low molecular weight fraction of dPSU-R, which is miscible with PA, interdiffused into the PA layer. A significant broadening of the interfacial profile was not observed as would be expected if any significant interdiffusion of the diblock copolymer into the PSU and PA layers had occurred. Therefore, it can be concluded that the diblock once formed stays localized at the interface, and builds up an interfacial concentration expressed in terms of the interfacial density (number of the block copolymers/unit of interfacial area). Unlike the examples of an added diblock as a third component or a recently reported graft system mentioned above, there is not substantial broadening of the interface.^{16,17,42,43} This allows the conclusion that the diblock, once formed, strongly aligns as a monolayer along the interface minimizing the interfacial free energy of the system. As we will discuss shortly, the presence of this layer which is critical for adhesion between the two immiscible polymers inhibits the formation of sufficient copolymer needed to exceed the critical threshold for z^*/R_g . Although the qualitative

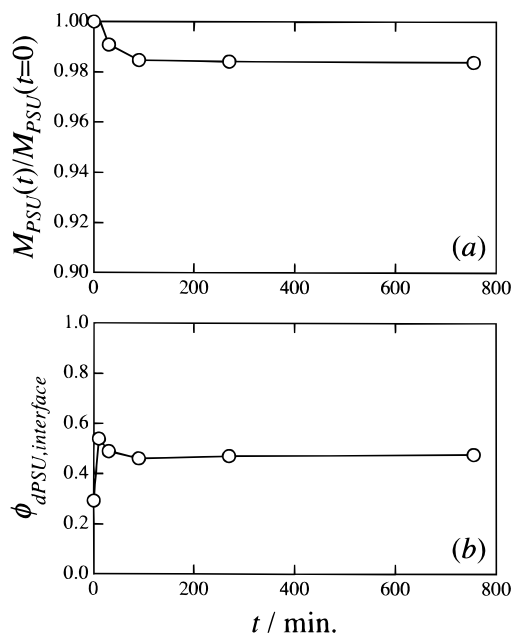


Figure 6. (a) Change in the integrated value for the SLD corresponding to PSU with annealing time, $M_{\text{PSU}}(t)$, normalized by the value before annealing, $M_{\text{PSU}}(t=0)$. (b) Change in the maximum volume fraction of dPSU in the interfacial region in the composition profile with annealing time. Both data are obtained for the diluted reactive system (Si//dPSU-R/hPSU//PA/air) in Figure 3.

behavior of the pure nonreactive system is similar to the reactive system, the pure nonreactive system exhibits a slightly but significantly smaller interfacial width of $W_{\text{I,obs}} = 30 \text{ \AA}$ than the pure reactive system, which is a reasonable value for immiscible polymer blends at high temperatures.¹⁻⁴

IV-3. Interfacial Coverage of the Diblock Copolymers Formed at the Interface. Having considered the pure reactive and nonreactive cases, some results for the diluted system can be interpreted as follows. Similar to the pure reactive or pure nonreactive system, the total mass of the PSU layer decreases after annealing at $T = 210 \text{ }^\circ\text{C}$ as seen in Figure 3c. Figure 6a provides a more quantitative demonstration of the time dependent change in the total mass of the PSU layer, $M_{\text{PSU}}(t)$, normalized by the total mass before annealing, $M_{\text{PSU}}(t=0)$ for the diluted reactive system. The normalized mass $M_{\text{PSU}}(t)/M_{\text{PSU}}(0)$ was estimated from the time dependent change in the SLD profile shown in Figure 3c. The mass rapidly decreases with time in the first 10 min of annealing and reaches an equilibrium value after ≈ 30 min of annealing, as a consequence of interdiffusion of low molecular weight species of hPSU and dPSU-R. However the amount of the decrease turns out to be very small (only $\approx 2.0\%$). This trend is identical to the pure reactive and nonreactive systems.

The increase of deuterated species at the interface after annealing, as seen in Figure 3c and Table 2, is clear evidence for diblock formation via an interfacial reaction. Initially, diblock formation causes an increase in volume fraction of dPSU species at the interface from 30 to 54 vol % with a layer thickness on the order of 110 to 130 \AA . Here ϕ_{dPSU} designates dPSU-R before reaction and dPSU blocks in dPSU-*b*-PA after reaction. There are two probable explanations for the observed thickness of the deuterium enriched layer. One of these assumes that this layer is composed of a monolayer of

the dPSU part of the dPSU-*b*-PA block copolymer (dPSU-brushes) formed and localized at the interface. Alternatively, the enriched layer could consist of the dPSU-brushes plus an enriched layer of dPSU-R adjacent to the dPSU-brushes. The thickness of the dPSU-brushes of dPSU-*b*-PA blocks are estimated to be about 112 \AA ($\approx 1.3R_g$ of dPSU-R, with $R_g = (Nl^2/6)^{1/2} \approx 86 \text{ \AA}$ (using $N = 61$ and $l = 27 \text{ \AA}$ ⁴⁸)). Thus, it is conceivable that the layer enriched by the deuterated species nearly corresponds to a monolayer of dPSU brushes since the total thickness of the enriched layer is 110–130 \AA . In terms of the normalized surface excess, z^*/R_g , z^* is defined as

$$z^* = \int_{520}^{670} (\phi(z) - 0.267) dz \quad (7)$$

Figure 3c indicates $z^*/R_g \approx 0.1\text{--}0.2$ for the diluted system, which is consistent with the narrow interfacial width and a positive interfacial tension.⁴²

Again, the time dependence of the SLD profile, Figure 3c, shows that the diffusion of the diblock (formed at the interface) from the interface into the PSU or the PA layer can be excluded on the basis of the same arguments mentioned above. Figure 6b shows the maximum volume fraction of deuterated species at the interface $\phi_{\text{dPSU,interface}}$ as a function of annealing time. The value $\phi_{\text{dPSU,interface}}$ is the maximum value of $\phi_{\text{dPSU-R}}(z)$ shown in Figure 3c. It increases from an initial value of 0.3 to a maximum value of 0.54 and eventually reaches an equilibrium value (designated $\phi_{\text{dPSU,interface}}^*$) of 0.47. The results shown in Figures 3c and 6b clearly indicate that the interfacial area is not fully covered by the block copolymers dPSU-*b*-PA, simply because the volume fraction $\phi_{\text{dPSU,interface}}^*$ does not reach a value of ≈ 1 . Although the interfacial reaction occurs, complete coverage of the interfacial area by dPSU-*b*-PA does not.

The interfacial width of the diluted reactive system is nearly identical to the value observed in the nonreactive system (Figure 4b). Two possible explanations for this behavior are considered. First, the molecular weights of the hPSU and dPSU-R in the diluted reactive system are greater than the molecular weight of dPSU in the pure nonreactive system (see Table 1). This increases the segregation power (χN) and the interfacial tension between PSU and PA phases in the diluted reactive system prior to reaction.^{4,5,49} Second, the fraction of the interfacial area covered by the block copolymers is about 50% ($\phi_{\text{dPSU,interface}}^* \approx 0.5$) leading to a small decrease of the interfacial tension. These two counterbalancing effects in the diluted reactive system relative to the pure nonreactive system (i.e., the molecular weight effect and the effect of block copolymer formation) provide a possibility that the net interfacial tension of the diluted reactive system is still approximately equal to the pure nonreactive system with the consequence of comparable interfacial widths in both systems.

In recent theoretical work¹⁸⁻²¹ analyzing interfacial reactions at the polymer/polymer interface, it was pointed out that the increasing interfacial density of block copolymer formed creates a barrier which inhibits the diffusion of the reactive end group labeled polymer still present in the bulk phase to the interface. A maximum critical interfacial density $\rho_s^* = 1/(l^2 N^{1/2})$ of diblocks is obtained when this diffusion barrier is on the order of kT . As soon as this critical interfacial density ρ_s^* is reached, the interfacial reaction is basi-

cally prevented as both reactive polymers must first penetrate the diblock brush at the interface before they can react. Interestingly, it can be shown following arguments given by Leibler⁵⁰ that diblocks present at a polymer/polymer interface only begin to significantly reduce the interfacial tension above an interfacial density of $\rho_s = 1/(N^{1/3}l^2)$ for the case of $\Delta\gamma/kT \approx 1$, since the reduction of interfacial tension scales with $\Delta\gamma/kT \approx (\rho_s l^2 N^{1/3})^3$. Therefore, at the maximum critical interfacial density of diblocks achieved during an interfacial reaction $\rho_s^* = 1/(l^2 N^{1/2})$, the reduction of surface tension is about $\Delta\gamma/kT \approx 1/N^{1/2}$, which is small.^{19–21} The conclusion is that it is impossible to obtain an interfacial coverage with diblocks big enough to significantly reduce the interfacial tension of a system through an interfacial reaction using diluted systems, which would then give rise to a significant increase of the interfacial width. The arguments given above also provide a good interpretation for the difference in the values $W_{I,obs}$ between the pure reactive and the diluted reactive system. On the other hand, recent reactive blending experiments using a graft system show a surface enrichment of formed graft block copolymer exceeding the critical threshold for z^*/R_g .^{16,17} It should be pointed out that their system is situated in the weak segregation regime whereas our systems show strong segregation.

IV-4. Remarks on Miscibility of dPSU–R and hPSU in the Diluted Reactive System. The arguments in section IV-3 a priori assume that dPSU–R and hPSU are miscible. However, as small modifications can significantly modify the miscibility of polymers due to the well-known low gain in combinatorial entropy upon mixing, it is very important to confirm if the polymer with reactive end group dPSU–R and the main matrix polymer hPSU in the diluted system are still miscible. To study the possibility that phase separation inside the mixed film of dPSU–R and PSU takes place and contributes in any way to the observed phenomena (e.g., triggers a segregation of the deuterated species), neutron scattering experiments have been performed to study the phase behavior of the mixture. These scattering experiments show that the mixture PSU–R/dPSU can be either miscible or phase separated, depending on the degree of polymerization (DP) of PSU in PSU–R.⁴⁸ We confirmed that the DP of the dPSU–R used here makes dPSU–R miscible with hPSU.

Besides small-angle neutron scattering (SANS) experiments, the bilayer interdiffusion experiments at 210 °C with neutron reflectivity as discussed earlier (Figure 5) indicate that both polymers used here form a completely miscible system, and it can be ruled out that phase separation between dPSU–R and PSU leads to any of the observed phenomena. Upon annealing, a preferential adsorption of deuterated species at the polymer/air interface is observed (Figure 5). The small differences between both polymers either due to the reactive end group or deuteration^{11,51–54} can lead to a preferential segregation of the dPSU–R to the air interface. In this case it is impossible to assign whether the end group or the isotope effect is causing this preferential adsorption of dPSU–R at the air interface.

IV-5. Separation of Contributions of $W_{I,diffuse}$ and $W_{I,capillary}$ to $W_{I,obs}$. The earlier mentioned contribution of capillary waves to the observed interfacial width can be estimated by calculating the intrinsic interfacial width using the segmental length l and the interaction parameter χ . The temperature dependence of the pa-

rameter χ is usually obtained by analyzing SANS data for a polymer blend in the single-phase state measured as a function of temperature according to the random phase approximation (RPA) equation.⁵⁵ Unfortunately, it is impossible to apply SANS to the present polymer pair since PSU and PA are almost completely immiscible in the experimentally accessible range of temperatures. Therefore, we have estimated χ from the temperature dependence of interfacial tension γ between PSU and PA according to the equation given by Helfand⁵

$$\gamma = l\rho_0 k_B T(\chi/6)^{1/2} \quad (8)$$

For simplicity, it is assumed that the segment length l and segmental density ρ_0 for the two homopolymers are equal. Furthermore, l is assumed to be $l = 27$ Å, which was obtained by analyzing SANS data for the dPSU/PSU–R mixture.⁴⁸ Additionally, the volume per segment $1/\rho_0 = 648$ Å³ is required. The γ 's obtained by the spinning drop method at 280 and 300 °C are 9.1 ± 0.7 and 7.5 ± 0.6 mN/m, respectively, for the pure nonreactive system (dPSU//PA). Using eq 8, the temperature dependence of χ was estimated as

$$\chi(T) = -4.696 + 2.871 \times 10^3/T \quad (9)$$

According to eqs 1 and 9, $W_{I,diffuse}$ between the dPSU and PA layer at 210 °C was estimated to be $W_{I,diffuse} \approx 20$ Å. As the calculated intrinsic interfacial width is smaller than the observed interfacial width $W_{I,obs}$ (37.0 Å), capillary wave fluctuations obviously contribute to $W_{I,obs}$ in the pure nonreactive system. By applying eq 6, $W_{I,capillary}$ is estimated to be about 31 Å. This effect has been frequently observed in thin film experiments^{1,2,46,56,57} and is quite large even for strongly incompatible systems. Hence, it is important to consider that effects of confined geometry may significantly alter the effect of capillary waves^{2,57} in thin films.

The above arguments are valid in the context of the strong segregation limit, i.e., the limit where $\chi N \rightarrow \infty$. In reality N is finite so that γ is smaller than the limiting value predicted from eq 8.^{1,2} Hence $W_{I,diffuse}$ is larger than the limiting value predicted from eq 1. As for the latter statement we note the relationship given by

$$W_{I,diffuse} = \frac{1}{3} l^2 \rho_0 k_B T \gamma^{-1} \quad (10)$$

from eqs 1 and 8. Since $W_{I,diffuse}$ increases when the small N effect is taken into account, $W_{I,capillary}$ is expected to become smaller than 31 Å. In fact we note

$$W_{I,capillary} \sim \gamma^{-1/2} \quad (11)$$

revealing an intriguing crossover of $W_{I,obs}$ from $W_{I,diffuse}$ dominance to $W_{I,capillary}$ dominance, with increasing γ or χ as will be discussed elsewhere.⁴⁰ Needless to say, reducing N is also important to the point that the system comes close to the weak segregation regime whereby the barrier of the diblock formed at the interface to the formation of new diblocks becomes weaker, resulting in the regime of $\gamma < 0$ where the interfacial instability occurs.¹⁶

These results, where a reactive blending mechanism is utilized to form diblock at the interface between two immiscible homopolymers, also show a striking differ-

ence compared to experiments where the diblock polymer was added separately as a third component. Adding different amounts of a diblock separately as a third component in the corresponding blend systems provides the possibility for the diblock to segregate to the homopolymer/homopolymer interface with high coverage and also to form micelles and other well-known structures inside each homopolymer phase.⁴³

V. Conclusions

The fundamental process of reactive blending of two incompatible polymers PSU and PA containing a reactive end group-labeled dPSU-R species was investigated using neutron reflectivity. The dPSU-R considered here has a phthalic anhydride end group that can react with the free amine end group of PA, forming a block copolymer dPSU-*b*-PA. In additional neutron reflectivity and SANS experiments, it was confirmed that the end group modified and isotopically labeled dPSU-R is still completely miscible with hPSU, which is used as the matrix polymer. This conclusion is consistent with the observation by Takeno et al.⁴⁸ Therefore, any effects of phase separation inside the mixed layer of hPSU/dPSU-R in the diluted system can be ruled out.

The results presented here show that the block copolymer formation takes place at the interface between the PSU and PA layers. The diblock stays localized at the interface and builds up an equilibrium coverage of 47 vol % at the interface. The diblock polymer forms a brush at the interface, which acts as a barrier to the diffusion of other reactive end-group-labeled polymer chains still present in the bulk phase toward the interface. Therefore, only a low interfacial coverage of $\phi^*_{\text{dPSU,interface}} = 0.47$ is observed. This coverage is too small to significantly reduce the interfacial tension in the system, explaining why the interfacial width in the pure nonreactive system and the diluted system are of similar and smaller magnitude than the pure reactive system. The block copolymer, once formed, remains localized at the interface and inhibits the formation of sufficient copolymer to obtain surface excesses large enough to eliminate the interfacial tension between immiscible PSU/PA. These results suggest that adding small amounts of reactive polymers during a reactive blending process may be enough to form sufficient copolymer to achieve the desired adhesion across the interface between two phases. Nevertheless, insufficient diblock polymer is formed to significantly decrease the interfacial tension or broaden the interfacial width.

Acknowledgment. T.H. and M.W. would like to gratefully acknowledge the German Ministry for Science (BMBF project 03N30283) for a partial financial support of this work. H.G. would like to thank the Alexander von Humboldt-Foundation for financial support.

References and Notes

- Genzer, J.; Composto, R. J. *Polymer* **1999**, *40*, 4223.
- Sferrazza, M.; Xiao, C.; Jones, R. A. L.; Bucknall, D. G.; Webster, J.; Penfold, J. *Phys. Rev. Lett.* **1997**, *78*, 3693.
- Stamm, M.; Schubert, D. W. *Annu. Rev. Mater. Sci.* **1995**, *25*, 325.
- Helfand, E.; Tagami, Y. *J. Chem. Phys.* **1972**, *56*, 3592.
- Helfand, E. *J. Chem. Phys.* **1975**, *62*.
- Dai, K. H.; Kramer, E. J.; Shull, K. R. *Macromolecules* **1992**, *25*, 5, 220.
- Shull, K. R.; Kramer, E. J.; Hadziioannou, G.; Tang, W. *Macromolecules* **1990**, *23*, 4780.
- Russell, T. P. *Curr. Opin. Colloid Interface Sci.* **1996**, *1*, 107.
- Kulasekere, R.; Kaiser, H.; Ankner, J. F.; Russell, T. P.; Brown, H. R.; Hawker, C. J.; Mayes, A. M. *Macromolecules* **1996**, *29*, 9, 5493.
- Russell, T. P.; Menelle, A.; Hamilton, W. A.; Smith, G. S.; Satija, S. K.; Majkrzak, C. F. *Macromolecules* **1991**, *24*, 4, 5721.
- Russell, T. P. *Annu. Rev. Mater. Sci.* **1991**, *21*, 249.
- Koriyama, H.; Oyama, H. T.; Ougizawa, T.; Inoue, T.; Weber, M.; Koch, E. *Polymer* **1999**, *40*, 6381.
- Triacca, V. J.; Ziaee, S.; Barlow, J. W.; Keskkula, H.; Paul, D. R. *Polymer* **1991**, *32*, 1401.
- Scott, C.; Macosko, C. J. *Polym. Sci., Part B: Polym. Phys.* **1994**, *32*, 205.
- Lyu, S. P.; Cernohous, J. J.; Bates, F. S.; Macosko, C. W. *Macromolecules* **1999**, *32*, 106.
- Jiao, J. B.; Kramer, E. J.; de Vos, S.; Moller, M.; Koning, C. *Macromolecules* **1999**, *32*, 2, 6261.
- Jiao, J. B.; Kramer, E. J.; de Vos, S.; Moller, M.; Koning, C. *Polymer* **1999**, *40*, 3585.
- Fredrickson, G. H.; Milner, S. T. *Macromolecules* **1996**, *29*, 9, 7386.
- Fredrickson, G. H. *Phys. Rev. Lett.* **1996**, *76*, 3440.
- O'Shaughnessy, B.; Sawhney, U. *Macromolecules* **1996**, *29*, 9, 7230.
- O'Shaughnessy, B.; Sawhney, U. *Phys. Rev. Lett.* **1996**, *76*, 3444.
- Weber, M.; Heckmann, W. *Polym. Bull.* **1998**, *40*, 227.
- Charoensirisomboon, P.; Saito, H.; Inoue, T.; Weber, M.; Koch, E. *Macromolecules* **1998**, *31*, 4963.
- Charoensirisomboon, P.; Chiba, T.; Solomko, S. I.; Inoue, T.; Weber, M. *Polymer* **1999**, *40*, 6803.
- Certain commercial materials and instruments are identified in this article to adequately specify the experimental procedure. In no case does such identification imply recommendation or endorsement by the National Institute of Standards and Technology, nor does it imply that materials or equipment identified are necessarily the best available for the purpose.
- Joly, R.; Bucourt, R.; Mathieu, J. *Recl. Trav. Chim.* **1959**, *78*, 527.
- Rueggeberg, W. H. C.; Sauls, T. W.; Norwood, S. L. *J. Org. Chem.* **1955**, *20*, 445.
- Russell, T. P. *Mater. Sci. Rep.* **1990**, *5*, 171.
- Welp, K. A.; Co, C. C.; Wool, R. P. *J. Neutron Res.* **1999**, *8*, 37.
- Birshtein, T. M.; Liatskaya, Yu. U.; Zhulina, E. Q. *Polymer* **1990**, *31*, 2185.
- Shibayama, M.; Hashimoto, T. *Macromolecules* **1986**, *19*, 9, 740.
- Hashimoto, T.; Nagatoshi, K.; Todo, A.; Hasegawa, H.; Kawai, H. *Macromolecules* **1974**, *7*, 364.
- Hashimoto, T.; Shibayama, M.; Kawai, H. *Macromolecules* **1980**, *13*, 3, 1237.
- Berk, N. F.; Majkrzak, C. F. *Phys. Rev. B* **1995**, *51*, 11296.
- Majkrzak, C. F.; Berk, N. F.; Dura, J. A.; Satija, S. K.; Karim, A.; Pedulla, J.; Deslattes, R. D. *Physica B* **1998**, *248*, 338.
- Majkrzak, C. F.; Berk, N. F.; Dura, J.; Satija, S. K.; Karim, A.; Pedulla, J.; Deslattes, R. D. *Physica B* **1997**, *241*, 1101.
- Hashimoto, T.; Tsukahara, Y.; Kawai, H. *J. Polym. Sci., Polym. Lett. Ed.* **1980**, *18*, 585.
- Boltzmann, L. *Ann. Phys.* **1894**, *53*, 960. Matano, C. *Jpn. Phys.* **1933**, *8*, 109.
- Schewmann, P. G. *Diffusion in Solids*; McGraw-Hill: New York, 1963; pp 28–32.
- Hayashi, M.; Hashimoto, T.; Gruell, H.; Esker, A.; Weber, M.; Satija, S. K.; Han, C. C. To be published.
- Thus the undulation has to be studied using either off-specular reflectivity, or real-space analysis with cross-sectional transmission electron microscopy and with atomic force microscopy on the specimens after removing the PA layer. These studies are beyond the scope of the present studies and deserve future work.
- Shull, K. R. *J. Chem. Phys.* **1991**, *94*, 5723.
- Shull, K. R.; Kellock, A. J.; Deline, V. R.; Macdonald, S. A. *J. Chem. Phys.* **1992**, *97*, 2095.
- Adamson, A. W.; Gast, A. P. *Physical Chemistry of Surfaces*, 6th ed.; John Wiley & Sons: New York, Chichester, England, Weinheim, Germany, Brisbane, Australia, Singapore, and Toronto, Canada, 1997.

- (45) Shull, K. R.; Mayes, A. M.; Russell, T. P. *Macromolecules* **1993**, *26*, 6, 3929.
- (46) Semenov, A. N. *Macromolecules* **1993**, *26*, 6, 6617.
- (47) The initial interfacial width of $W_{l,obs} = 5 \text{ \AA}$ for the as-prepared bilayers is a nonequilibrium interfacial width and artificially narrow, as it represents essentially the surface roughness of the single layers of PA and polysulfones (either dPSU-R, dPSU, or dPSU-R/hPSU). The surface roughness of the PA layer attached to the Si wafer used is as smooth as that of the Si wafer itself, and the surface roughness of the polysulfones/air was measured to be $W_{l,obs} = 3.3 \text{ \AA}$ by X-ray reflectivity. Thus the thin initial width of $W_{l,obs} = 5 \text{ \AA}$ seems to be a reasonable value as a roughness between the two contacting films. In fact the 5 \AA roughness is consistent with a well spin-coated film regardless of the polymer and solvent used.
- (48) Takeno, H.; Hashimoto, T.; Weber, M.; Schuch, H.; Koizumi, S. *Polymer* **2000**, *41*, 1309.
- (49) Schubert, D. W.; Stamm, M. *Europhys. Lett.* **1996**, *35*, 419.
- (50) Leibler, L. *Makromol. Chem.—Macromol. Symp.* **1988**, *16*, 1.
- (51) Krausch, G. *Mater. Sci. Eng. R—Rep.* **1995**, *14*, 1.
- (52) Kumar, S. K.; Russell, T. P. *Macromolecules* **1991**, *24*, 4, 3816.
- (53) Hariharan, A.; Kumar, S. K.; Russell, T. P. *J. Chem. Phys.* **1993**, *98*, 4163.
- (54) Hariharan, A.; Kumar, S. K.; Russell, T. P. *Macromolecules* **1991**, *24*, 4, 4909.
- (55) de Gennes, P. G. *Scaling Concepts in Polymer Physics*; Cornell University, New York, 1979.
- (56) Hermes, H. E.; Higgins, J. S.; Bucknall, D. G. *Polymer* **1997**, *38*, 985.
- (57) Kerle, T.; Klein, J.; Binder, K. *Phys. Rev. Lett.* **1996**, *77*, 1318.

MA000109R